High-Power Vertical-Cavity Surface-Emitting Laser Pump Sources

Jean-Francois Seurin, Guoyang Xu, James D. Wynn, Dennis Tishinin, Qing Wang, Viktor Khalfin, Alex Miglo, Prachi Pradhan, L. Arthur D'Asaro, and Chuni Ghosh

Abstract

This work presents recent results on high-power, high-efficiency two-dimensional vertical-cavity surface-emitting laser (VCSEL) arrays emitting around 980 nm. More than 230 W of continuous-wave (CW) power is demonstrated from a ~5 mm x 5 mm chip. In quasi-CW mode, smaller chips exhibit 100 W output power, corresponding to more than 3.5 kW/cm^2 of power density. We show that many of the advantages of low-power single VCSEL devices such as reliability, wavelength stability, low-divergence circular beam, and low-cost manufacturing are preserved for these high-power arrays. VCSELs thus offer an attractive alternative to the dominant edge-emitter technology for high-power pumping.

Introduction

Compact and robust high-power semiconductor lasers are needed in a variety of industrial, medical, and defense applications, foremost among them the pumping of solid-state and fiber lasers. Currently, the dominant technology is that of edge-emitting semiconductor lasers. However, this technology has the disadvantages of low array reliability, an elliptical beam profile, and poor wavelength stability. Furthermore, upward scaling of the output power requires complex and costly assembly of edge-emitting bars into stacks. In the case where collimating and/or wavelength stabilizing optics are required, the complexity of the assembly process increases further.

The vertical-cavity surface-emitting laser (VCSEL) technology presents an attractive alternative as a high-power (several hundred Watts) semiconductor laser source because it can be easily processed in 2D arrays to scale up the power {1}. Ironically, VCSELs' rise to fame originated in "low-power" (sub-milliwatt) applications during the mid-90s {2}. This success was mainly due to the lower manufacturing costs and higher reliability of VCSELs compared to edge-emitters. This work presents recent advances on high-power VCSEL 2-D arrays and shows that many key features of single VCSEL devices are preserved for these high-power arrays.

First, we go over the design and fabrication details. We then present recent results: using a relatively small VCSEL 2-D array (~0.22 cm^2 area), we have demonstrated more than 230 W of continuous-wave (CW) output power, corresponding to more than 1 kW/cm^2 power density. We have also demonstrated 100 W from quasi-CW (QCW) small arrays (~0.028 cm^2 area), corresponding to more than 3.5 kW/cm^2 power density. These arrays emit at around 980 nm. To the best of our knowledge, these CW and QCW power levels represent record results for 2-D VCSEL arrays. Finally, we go over some of the main advantages of these high-power VCSEL arrays in terms of reliability, and spectral and beam properties.

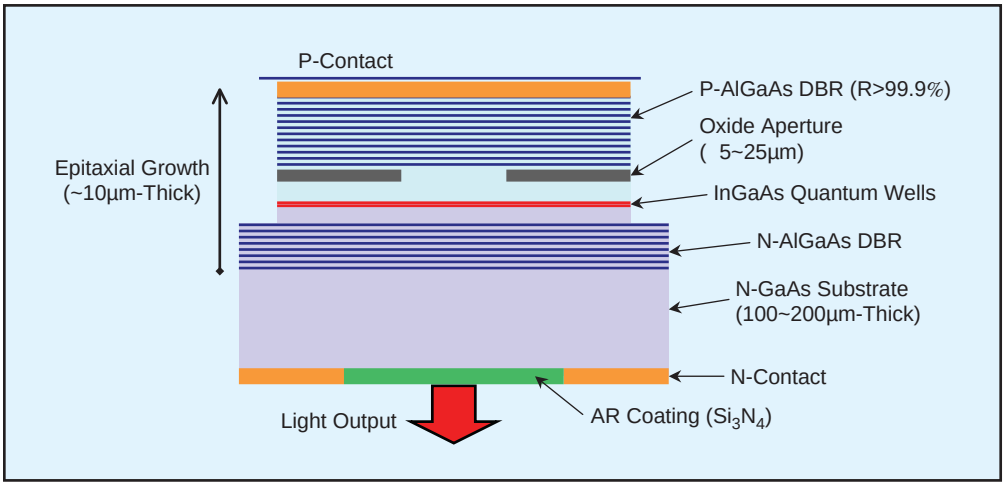

Figure 1: Schematic cross-section (not to scale) of a bottom-emitting 980 nm vertical-cavity surface-emitting laser structure. The active region typically comprises 1~4 InGaAs quantum wells, embedded in a one-wavelength-thick AlGaAs cavity. The cavity is sandwiched between two distributed Bragg reflector stacks (DBRs) consisting of alternating high and low refractive index quarter-wavelength layers. The reflectivity of these DBRs is in the range 99.5 - 99.9% for the output mirror and >99.9% for the back mirror. Current and/or mode confinement can be achieved by selective oxidation of an Aluminum-rich layer located near the active region. Light emission is through the transparent GaAs substrate. A Si_3N_4 anti-reflection (AR) coating is deposited at the substrate/air interface.

PRINCETON OPTRONICS, INC.,1 ELECTRONICS DRIVE, MERCERVILLE, NJ 08619

Structure design

The design of high-power 2-D VCSEL arrays derives from the design of efficient single-devices. Our single device VCSEL structure is based on a selectively oxidized, bottom-emitting design as shown in Figure 1.

The selective oxidation process {3} provides efficient optical mode and injection current confinement and greatly improves the performance of the device since the oxidized material is electrically insulating and has a lower refractive index than the semiconductor material {4}. The bottom-emitting configuration (also referred to as "junction-down") is necessary for efficient heat-sinking and more uniform current injection {5}. Indeed, using such mounting configuration, we have previously achieved record 3 W output power at room temperature under CW operation from single devices with large apertures {6}. The devices used in large arrays have lower output powers (10-100mW, depending on aperture size) with high conversion efficiency. By combining 1000~10 000 such devices in parallel in a two-dimensional array, very high powers can be achieved while maintaining high conversion efficiency.

The epitaxial structure is grown using MOCVD on 3" GaAs n-doped (Silicon) substrates. The structure consists of InGaAs quantum wells in a one-wavelength cavity, sandwiched between Carbon-doped and Silicon-doped AlGaAs distributed Bragg reflectors (DBRs). A thin, Aluminum-rich AlGaAs layer is placed at the bottom of the p-DBR near the active region for subsequent oxidation to form an optical and electrical aperture.

The structure is optimized for high wall-plug efficiency in mainly two ways. First, the doping profiles in the DBRs are carefully designed to minimize optical absorption while maintaining satisfactory electrical conductivity {7}. Second, the reflectivity of the output n-DBR is optimized to obtain the highest slope efficiency while maintaining a reasonable threshold current. Decreasing the output reflectivity will increase the slope efficiency but will also increase the threshold current. At some point heating at threshold will be excessive and the slope efficiency will cease to increase (and even start to decrease) with further reduction of the output mirror reflectivity {8}.

Implementation of these design optimizations resulted in a record 51% conversion efficiency for bottom-emitting 980 nm single VCSEL devices, as shown in Figure 2. This level of performance is comparable to that already achieved for top-emitting 980 nm VCSELs {9}.

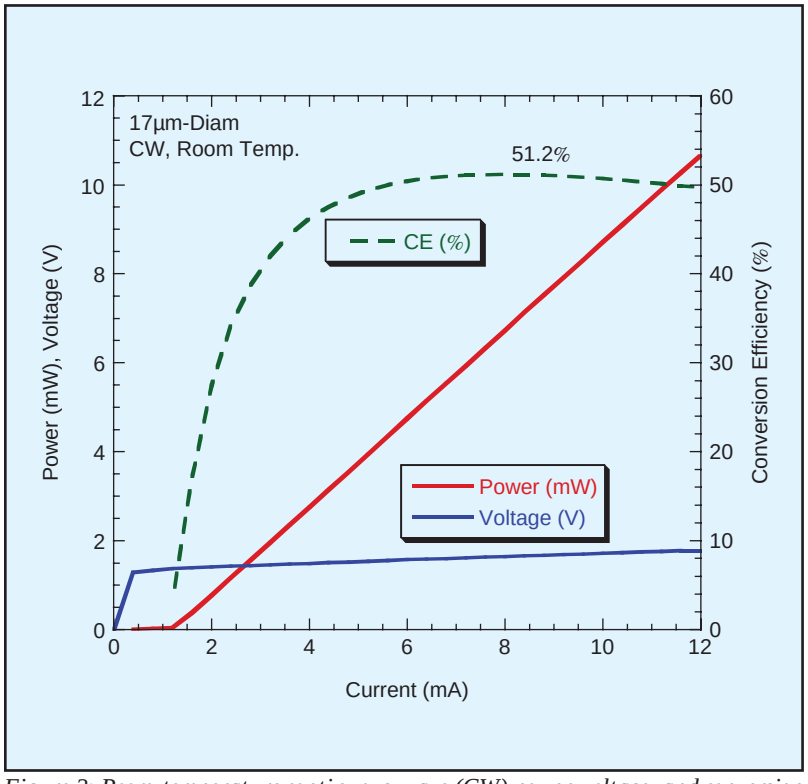

Figure 2: Room-temperature continuous-wave (CW) power, voltage, and conversion efficiency of an electrically injected bottom-emitting 980 nm VCSEL device. The aperture is defined by selective oxidation and is 17 µm in diameter. The conversion efficiency reaches a maximum of 51.2% at 8 mA.

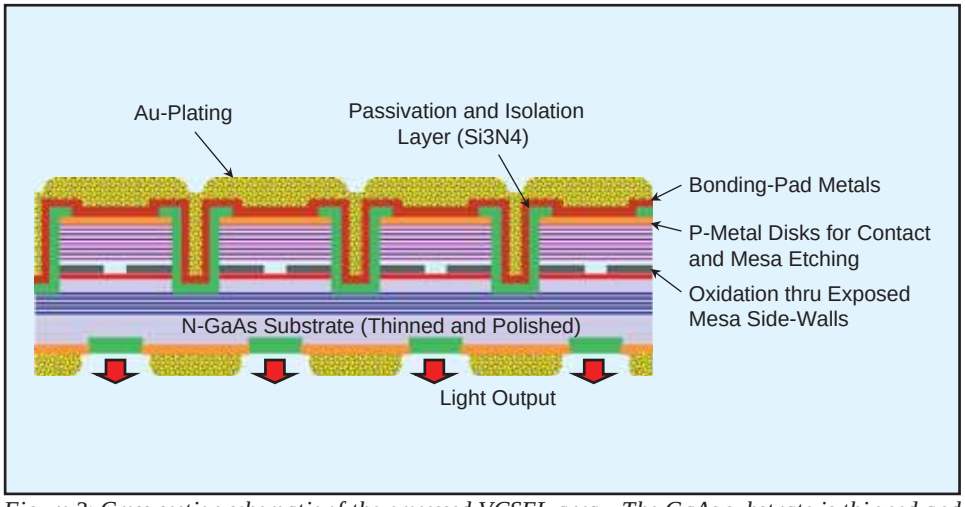

Figure 3: Cross-section schematic of the processed VCSEL array. The GaAs substrate is thinned and polished to an optical finish, followed by the deposition of a quarter-wavelength Si_3N_4 layer (AR coating) and patterned evaporated metals to form the n-contacts and emission windows. Individual devices are defined by reactive-ion etching (RIE) of individual mesas followed by selective oxidation to form electrically conducting apertures. The p-contact disks serve as the RIE mask. The epitaxial surface is then passivated with a Si_3N_4 layer. Windows are then opened by patterned etching of the nitride, followed by e-beam evaporation of Ti/Pt/Au metals to form the bonding pad. Both the n-metals and bonding pad are electro-plated with Gold to improve current distribution across the array.

Array fabrication

Processing of the epitaxial material into 2-D VCSEL arrays follows the same standard, well-establish processing techniques that have been used for selectively oxidized single VCSEL devices for some time now (see {1} for example). A cross-section schematic of the processed sample is shown in Figure 3. Plating of the n- and p-contacts is required for uniform current distribution within the array.

We found that our selective oxidation process was extremely uniform within an array and among arrays within the same sample. Thus, we believe the selective oxidation process is well suited for the production of VCSEL arrays even larger than 5mm x 5mm.

These arrays are tested at the wafer level (before cleaving and separation) to check for performance and excessive "dead pixels" for example. It is noteworthy that VCSEL array fabrication is identical to the well-established, low-cost silicon integrated-circuit planar processing. Since VCSELs are grown, processed and tested while still in the wafer form, there is significant economy of scale resulting from the ability to conduct parallel device processing, whereby equipment utilization and yields are maximized and set-up times and labor content are minimized. Furthermore, the wafers can be diced into single devices or arrays of different shapes and sizes. Depending on the application the arrays can be linear (1D), rectangular or square (2D). Furthermore, since the position of the individual elements in a VCSEL array is defined by photolithography, arbitrary design layouts of the elements with placement accuracy at the micron level are possible.

After cleaving and sorting, individual arrays are soldered onto metallized high-thermal-conductivity submounts such as diamond or BeO. Then, the chip-on-submount can be packaged onto a micro-channel cooler to increase the heat removal capacity, especially for CW operation. Figure 4 shows a ~5 mm x 5 mm VCSEL array chip fully packaged on a micro-channel-cooler.

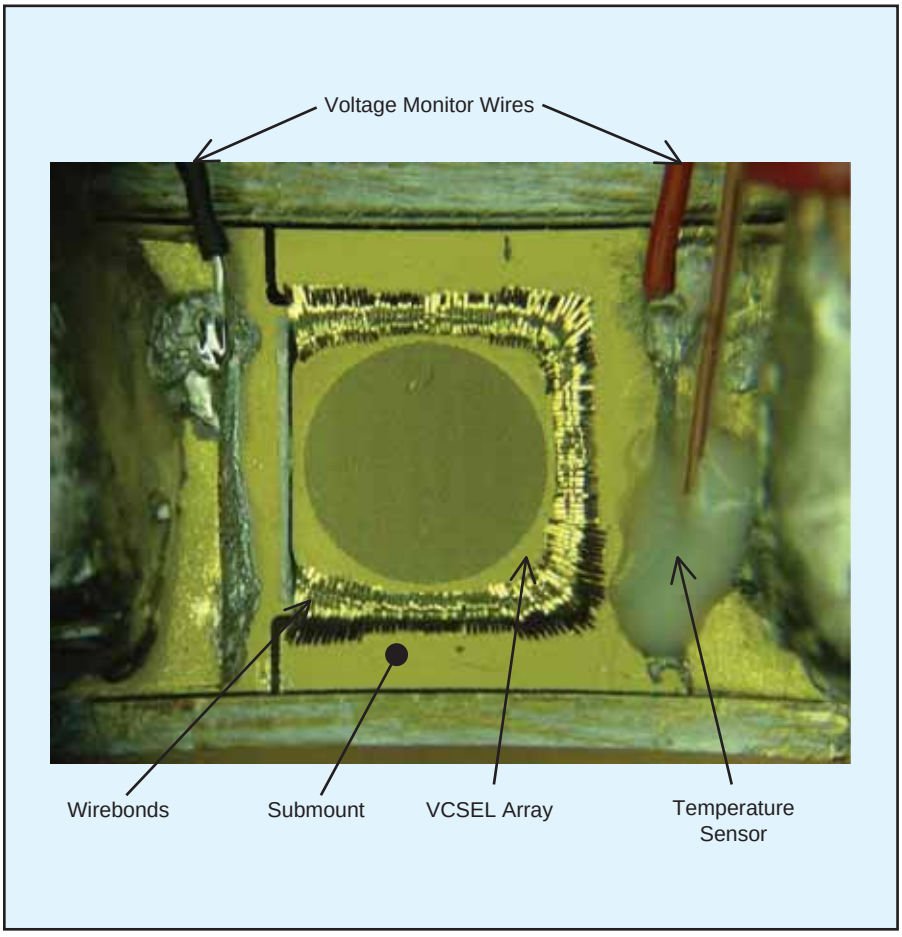

Figure 4: Photograph of a fully assembled 2-D VCSEL array on a diamond submount and micro-channel-cooler for CW testing. The VCSEL chip size is approximately 5 mm x 5 mm.

Array results

Figure 5(a) shows the CW LIV characteristics of an array packaged on a micro-channel-cooler similar to the one shown in Figure 4. This array has an emission area of ~0.22 cm^2 and was operated at a constant heat-sink temperature (15°C). A record 231W output power was reached with 320 A drive current, limited by thermal roll-over. This corresponds to a power density of 1 kW/cm2, similar to that achieved by CW high-power edge-emitter stacks. This array has a peak conversion efficiency >44%. Lower-power arrays (90 W maximum power) have been recently fabricated with conversion efficiencies at 51%, identical to that of single devices.

Smaller arrays were soldered on submounts and tested in QCW mode. The chip-on-submounts were not packaged on a micro-channel-cooler. Instead, they were tested on a TEC-controlled stage maintained at 20°C. Figure 5(b) shows the LIV characteristics of a 0.028 cm^2 array. Pulse-width and duty-factor were 100μs and 0.3%, respectively. Maximum power reached was 100 W, limited by the QCW current driver (125A), although some early signs of rollover are evident. This corresponds to a power density of 3.5 kW/cm^2, also similar to what is achieved with edge-emitter stacks. Higher power levels can be achieved by connecting several chips in series.

We also examined the spectral and beam properties of the array of Figure 5(a) at a 100W CW output power. Figure 6(a) shows the emission spectrum of this array. The spectral full-width half-maximum (FWHM) is only 0.8 nm, about one-fifth that of edge-emitter bars or stacks (typically in the 3 to 5 nm range). We also measured the wavelength shift as a function of the heat-sink temperature to be 0.065 nm/K, identical to the value for sin-

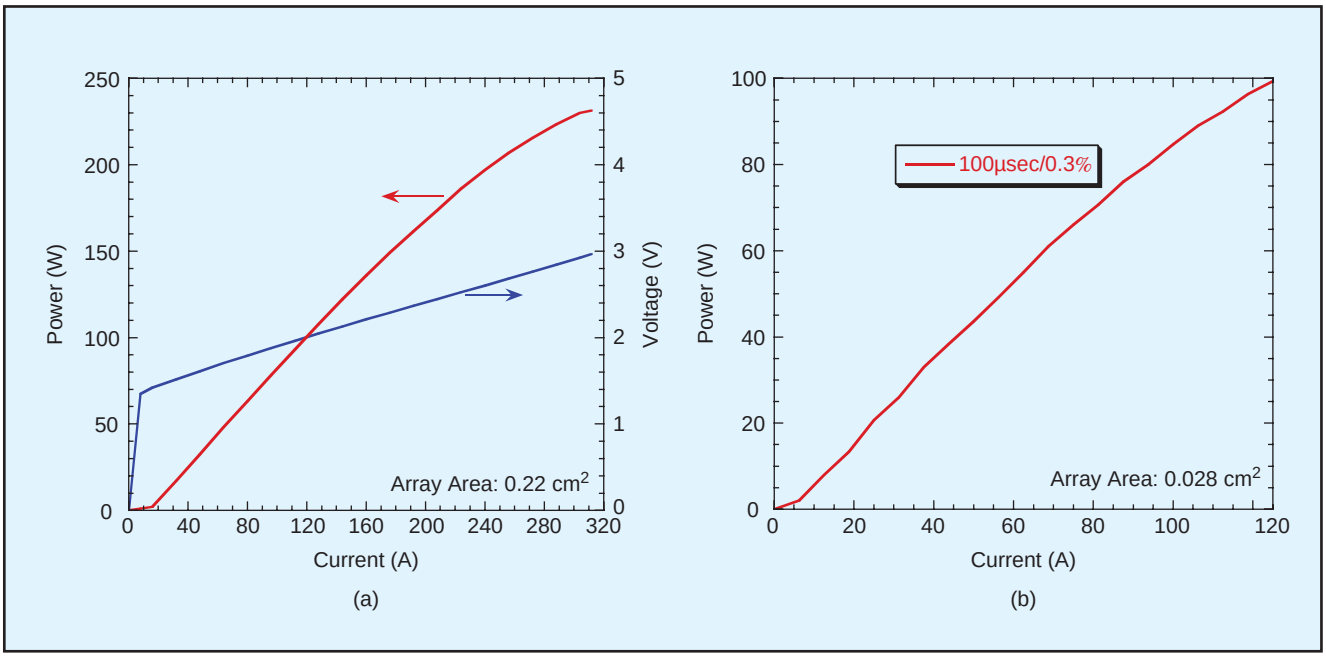

Figure 5: (a) CW output power and voltage of a 2-D VCSEL array assembled on a micro-channel-cooler. The VCSEL chip size is approximately 5 mm x 5 mm and is maintained at a constant heat-sink temperature of 15°C. A maximum power of 231 W at 320 A is reached, limited by thermal roll-over. This power level corresponds to a power density of 1 kW/cm^2 for this array. (b) QCW output power of a smaller (~0.028cm^2 area) 2-D VCSEL array. The pulse width and duty cycle are 100 µs and 0.3%, respectively. The array is tested on a TEC-controlled stage maintained at 20°C. The array reaches a maximum power of 100 W, limited by the current driver (125A max). This power level corresponds to a power density of 3.5kW/cm^2.

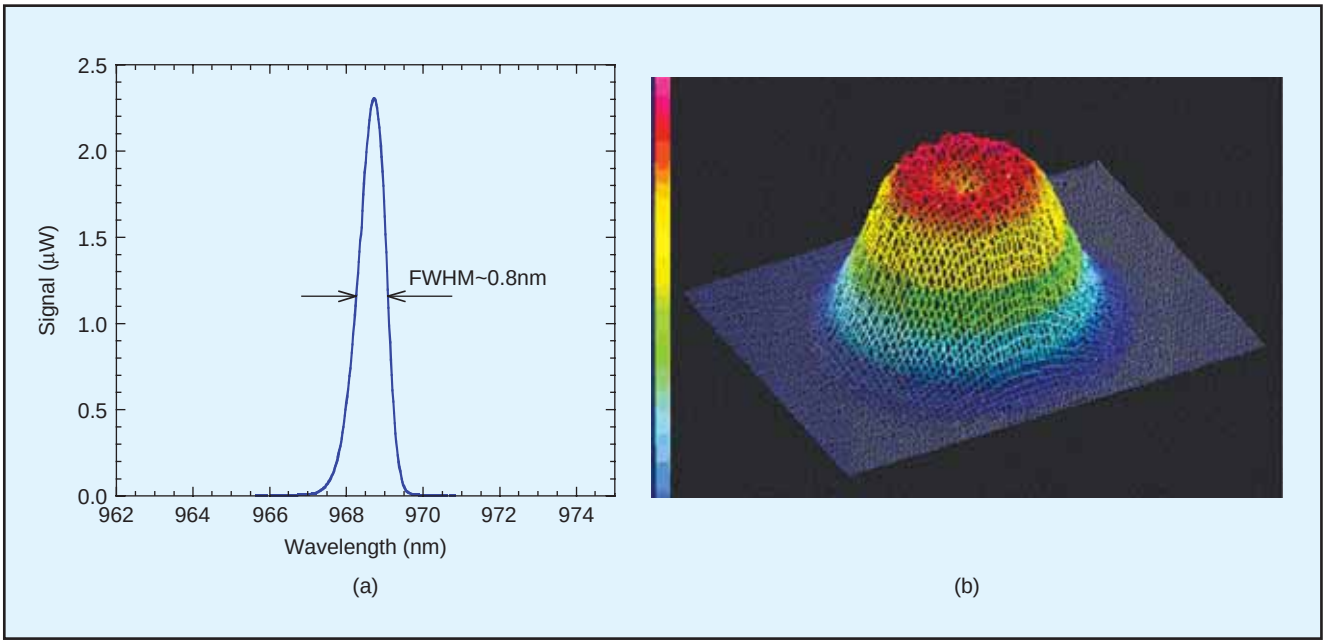

Figure 6: (a) Emission spectrum and (b) far-field beam distribution at a 100 W CW output power (~120A) for the array tested in Figure 5(a). At 100W, the array lases around 969 nm and has a spectral full-width half-maximum of 0.8 nm. The output beam is circular, with a "quasi-top-hat" distribution, and a 1/e^2 full-width divergence angle of 17°.

gle devices. This value is also one-fifth that of edge-emitters (typically 0.33 nm/K). Therefore, similarly to single devices, high-power VCSEL arrays benefit from an intrinsically narrow spectrum and stable emission wavelength. This is useful for many pumping applications where the medium has a narrow absorption band.

Figure 6(b) shows the intrinsic far-field beam profile of the array. The beam is circular, with a quasi-top-hat profile. The 1/e^2 full-width divergence angle is 17°. Since such beam characteristics can be achieved without any optics, VCSEL arrays present a cost-effective solution for end-pumping applications.

VCSEL reliability

In terms of reliability, VCSELs have an inherent advantage over edge-emitters because they are not subject to catastrophic optical damage (COD). For edge-emitters, this failure mechanism is very sensitive to the quality of the emission facet coating as well as junction temperature. This problem of sensitivity to surface conditions for edge-emitters is not present in VCSELs because the gain region is embedded in the epitaxial-structure and does not interact with the emission surface, and because the power densities involved are much smaller. Over the years, several reliability studies for VCSELs have yielded failures-in-time (FIT) rates (number of failures in one billion device-hours) on the order of 10 or less {10}, whereas FIT rates for telecom-grade edge-emitters is on the order of 500 {11}. The failure rate for industry-grade high-power edge-emitter bars or stacks is generally worse.

This VCSEL reliability advantage is very important for laser systems, where the end-of-life and field failures are overwhelmingly dominated by pump-laser failure. This also means that VCSELs can be reliably operated at higher temperatures {12}. This advantage is significant because the requirements for refrigeration become much less for VCSELs, resulting in a more compact laser system with higher overall efficiency.

Conclusions

We have shown that it is possible to use VCSEL technology to make compact high-power pump sources. Record CW (230 W) and QCW (100 W) power levels have been demonstrated from 2-D VCSEL arrays. Moreover, power density levels are comparable to those of edge-emitter stacks.

It was also shown that many of the advantages on which low-power single VCSEL devices built their success are preserved for these high-power VCSEL arrays. These advantages include low manufacturing costs, spectral stability and beam quality. Although the conversion efficiency of VCSELs has improved significantly in recent years (~51%), it still lags a bit behind that of edge-emitters (55~60% for commercial products). Still, since VCSELs can operate reliably at high temperature, the overall system efficiency could be higher using VCSELs since a refrigeration apparatus would not be needed.

Therefore, because of their significant and unique advantages in terms of costs, reliability, and performance VCSELs could become the next technology of choice for compact and efficient high-power semiconductor laser sources. In the near future, we plan to increase the VCSEL array CW and QCW power densities to 2 kW/cm^2 and 6 kW/cm^2, respectively. Work to improve the conversion efficiency is also ongoing.

Acknowledgements

The authors are grateful for the support from the DARPA Super High Efficiency Diode Source program (SHEDS).

References

[1] M. Grabherr et al, "Bottom-emitting VCSEL's for high-CW optical output power," IEEE Photon. Technol. Lett., Vol. 10, No. 8, pp. 1061-1063 (August 1998).

[2] K. S. Giboney et al, "The ideal light source for datanets," IEEE Spectrum, Vol. 35, No. 2, pp. 43-53 (February 1998).

[3] J. M. Dallesasse et al, "Hydrolyzation oxidation of AlxGa1-xAs-AlAs-GaAs quantum well heterostructures and superlattices," Appl. Phys. Lett., Vol. 57, No. 26, pp. 2844-2846 (December 1990).

[4] D. L. Huffaker et al, "Native-oxide defined ring contact for low threshold vertical-cavity lasers," Appl. Phys. Lett., Vol. 65, No. 1, pp. 97-99 (July 1994).

[5] R. Michalzik et al, "High-power VCSELs: modeling and experimental characterization," Proc. SPIE, Vol. 3286, pp. 206-219 (April 1998).

[6] L. A. D'Asaro et al, "High-power, high efficiency VCSELs pursue the goal," Photonics Spectra, pp. 64-66 (February 2005).

[7] M. G. Peters et al, "Growth of beryllium doped AlxGa1-xAs/GaAs mirrors for vertical-cavity surface-emitting lasers," J. Vac. Sci. Technol. B, Vol. 12, No. 6, pp. 3075-3083 (Nov/Dec 1994).

[8] G. M. Yang et al, "Influence of mirror reflectivity on laser performance of very-low-threshold vertical-cavity surface-emitting lasers," IEEE Photon. Technol. Lett., Vol. 7, No. 11, pp. 1228-1230 (November 1995).

[9] K. L. Lear et al, "Selectively oxidized vertical cavity surface emitting lasers with 50% power conversion efficiency," Electron. Lett., Vol. 31, No. 3, pp. 208-209 (February 1995).

[10] J. A. Tatum et al, "Commercialization of Honeywell's VCSEL Technology," Proc. SPIE, Vol. 3946, pp. 2-13 (May 2000).

[11] H.-U. Pfeiffer et al, "Reliability of 980 nm pump lasers for submarine, long-haul terrestrial, and low cost metro applications," Optical Fiber Communication Conference and Exhibit, OFC 2002, pp. 483-484 (March 2002).

[12] R. A. Morgan et al, "200∞C, 96-nm wavelength range, continuous-wave lasing from unbonded GaAs MOVPE-grown vertical cavity surface-emitting lasers," IEEE Photon. Technol. Lett., Vol. 7, No. 5, pp. 441-443 (May 1995).